Remote Sensing in Ecology and Conservation

Zoological Society of London

RESEARCH ARTICLE OPEN ACCESS

Development and Evaluation of a Low-Cost, Semi-Automated Camera Trap for Surveying Bumble Bee Communities

Michael P. Getz[1,2] | Lincoln R. Best[1] | Oksana Ostroverkhova[3] | Andony P. Melathopoulos[1] | Timothy L. Warren[1]

[1]Department of Horticulture, Oregon State University, Corvallis, Oregon, USA | [2]National Council for Air and Stream Improvement, Inc., Corvallis, Oregon, USA | [3]Department of Physics, Oregon State University, Corvallis, Oregon, USA

Correspondence: Timothy L. Warren (tim.warren@oregonstate.edu)

Received: 16 December 2025 | **Revised:** 25 May 2026 | **Accepted:** 23 June 2026

Keywords: Bombus | deep learning | diurnal insects | nonlethal insect monitoring | object detection | pollinator

ABSTRACT

Widespread declines in insect diversity and abundance underscore an urgent need for standardized, nonlethal monitoring methods for important pollinators such as bumble bees (*Bombus* spp.). Camera traps are widely used for nonintrusive, continuous surveys of large animals but have not yet been extensively adopted for monitoring diurnal insects. Automated camera traps could improve current insect survey methods, which often rely on lethal traps or in-person observation. Here we developed an open-source, low-cost camera trap for monitoring wild insects and evaluated its performance relative to established sampling approaches. We used a low-power microcomputer to collect time-lapse images on colored platforms that served as non-rewarding visual lures. We compared the performance of whole-image and tiled deep-learning models for automated detection of small insects in images captured by the traps. We found that tiled inference—which performs detection inside subframes of the original image—significantly improved accuracy, even outperforming human reviewers. Bumble bee visitation was highest on platforms with a repeating fluorescent bullseye pattern. Via continuous monitoring, the camera traps recorded bumble bee visits during all daylight hours over 18 days. From the recorded images, expert human taxonomists identified six *Bombus* species, yielding community composition and diversity estimates comparable to those obtained by hand netting. We simulated the effect of deploying variable numbers of cameras at sites with two levels of diversity. These simulations suggested that adding cameras substantially increased sampling completeness, particularly in species-rich communities. By pairing low-cost, semi-automated camera traps with deep-learning image analysis, our work provides a foundation for scalable, nonlethal studies of bumble bee diversity and activity patterns.

1 | Introduction

There is considerable evidence of recent, worldwide declines in the diversity and abundance of insects (Sánchez-Bayo and Wyckhuys 2019; Van Der Sluijs 2020; Wagner 2020). Of particular concern are North American and European native bees, especially bumble bees (*Bombus* spp.), which are effective and economically important diurnal pollinators (Biesmeijer et al. 2006; Cameron et al. 2011; Cameron and Sadd 2020; Jacobson et al. 2018). For many native bees, however, trends in range and abundance are not well understood; even at a coarse scale of 220 × 220 km, reliable inventory data exist for fewer than 40% of bee species in the United States (Chesshire et al. 2023). These gaps reflect limitations of conventional monitoring, which often involves temporally and spatially sparse sampling and can therefore be biased and poorly suited for

detecting rare species or community changes (Eeraerts and Meeus 2025; Graves et al. 2020; McNeil et al. 2019; Williams et al. 2001). Moreover, conventional monitoring typically relies on invasive specimen handling methods that cause mortality or sublethal harm, and are often prohibited for species of concern. These limitations motivate the need for more automated, nonlethal approaches to bumble bee monitoring.

Camera-based systems show potential for standardized, nonlethal insect monitoring. In larger animals, cameras often trigger image capture with passive infrared sensors, which are less reliable for small, ectothermic insects (Boom et al. 2014; Rovero et al. 2013; Rowcliffe et al. 2014; Samejima et al. 2012). Continuous, scheduled imaging is suitable for insects but generates large volumes of data without specimens (Droissart et al. 2021; Naqvi et al. 2022). To address this problem, recent studies have developed deep learning detection models to localize insects, often using simplified backgrounds, such as immobile, low-lying plants (Bjerge et al. 2022) or stationary, visually attractive lures (Künast et al. 2026; Sittinger et al. 2024; Teixeira et al. 2023). Object detection models have achieved high accuracy across multiple insect groups (Bjerge et al. 2025, 2023; Künast et al. 2026; Sittinger et al. 2024) but may not generalize to different camera platforms or taxa. Specialized detection methods for small objects, such as Slicing Aided Hyper Inference (SAHI)—which tiles each image into smaller frames for analysis—may aid insect detection (Akyon et al. 2022; Ye et al. 2024); however, it is unclear whether potential performance gains merit the added computational effort required.

Bumble bees are ideal targets for obtaining species-level data from camera trap images given their relatively large size, recognizable markings, and ecological significance. Many bumble bee species can be identified on the basis of high-quality dorsal images, either by human taxonomists or deep learning classification models (Colgan et al. 2024; Sittinger et al. 2024; Spiesman et al. 2021). However, there are known cryptic species pairs (e.g., *B. vosnesenskii* and *B. caliginosus*) that are not differentiable without direct examination. Few studies have tested whether camera traps can reliably produce images of sufficient quality to permit human taxonomists to classify bumble bee to species (c.f. Sittinger et al. 2024), which is a necessary step toward fully automated classification.

To survey bumble bees, or any insect community, a passive trap must attract as many species as possible. Light traps are highly effective for nocturnal insects such as moths (Montgomery et al. 2021; Roy et al. 2024), but attracting diurnal insects, which rely on color to select targets, is more challenging. Certain colors and patterns are known to attract bumble bees. For example, lethal blue vane traps are highly attractive to *Bombus* spp. (Hall 2018; Rao and Ostroverkhova 2015; Stephen and Rao 2005), owing in part to the traps' fluorescence and reflectance at 430 nm, aligned with the peak sensitivity of bee photoreceptors (Ostroverkhova et al. 2018). Many plants attract bumble bees via UV-reflective signals, including a concentric bullseye pattern, indicating pollen availability or potential floral rewards (Gronquist et al. 2001; Guldberg and Atsatt 1975; Koski and Ashman 2014). The contrast between floral patterns and the background may further allow bees to identify targets (Hempel De Ibarra et al. 2022; Van Der Kooi et al. 2019). The observed efficacy of blue vane traps and high-contrast floral guides suggests that combining these cues in a blue-fluorescent bullseye pattern on a platform lure could attract bumble bees.

The extent to which camera systems can survey bee communities is not well understood. There are substantial differences in bee community estimates obtained by blue vane traps, pan traps, and hand netting. Netting and vane traps tend to overrepresent *Bombus* spp., whereas pan traps more often collect small halictids (Boyer et al. 2020; Mathis et al. 2024; Wilson et al. 2008). Vane traps of different colors attract distinct *Bombus* species (Acharya et al. 2021). Such discrepancies highlight the need to validate community estimates obtained by camera traps, using methods that account for unequal sampling effort (Chao et al. 2020; Westphal et al. 2008).

In this study, we developed an open-source, semi-automated camera trap system that tracked bumble bee visitation to platforms with varying color and fluorescence. We found that a tiling approach significantly improved automated detection of bumble bees and other insects. We observed that bumble bees visited a fluorescent, repeating bullseye platform variant more than alternatives with single, solid colors. Our system estimated the diversity of bumble bee communities as effectively as hand netting, without destructive sampling. Our results provide a generalizable framework for further development of camera systems for nonlethal bee monitoring.

2 | Materials and Methods

2.1 | Camera Traps for Pollinator Monitoring

We constructed 10 camera traps using readily available materials at a per-unit cost of ~ USD $227 (2024 cost; bill-of-materials included as Data S1). The traps were controlled by low-power (~1–1.5 W) Raspberry Pi Zero or Zero 2 W computers (Raspberry Pi Foundation, Cambridge, United Kingdom), which ran Bullseye 64-bit Lite from a 64 GB Secure Digital (SD) card (SanDisk, Milpitas, CA, USA). A 19,200 mAh Voltaic Systems V75 battery in a dry bag provided power; a Witty Pi 4 Mini controlled startup and shutdown (Voltaic Systems, Brooklyn, NY, USA; Dun Cat B.V., Elst, NL). We connected an OLED display (Zhong JinYuan Technology, Henan, CN) for live status readout, and a precision real-time clock (Adafruit, Brooklyn, NY), for maintaining time across power outages, to the Pi via a SparkFun Qwiik Hat (SparkFun, Niwot, CO). The electronics were housed in a weatherproof box mounted to an inverted L-shaped aluminum frame. We placed the Pi Camera Module 3 (Raspberry Pi Foundation, Cambridge, United Kingdom) in a protective case, which we mounted to the top arm of the frame and pointed down at the platform lure (Figure 1A). We clamped the frame to a 61 cm rebar stake, which was hammered into the ground.

We replaced SD cards and batteries roughly every 48 h. Imaging occasionally paused due to hardware malfunctions, adverse weather, or delayed site visits. All traps initially used the Pi Zero computer, imaging at 0.5 frames per second (fps). We upgraded two traps to the Pi Zero 2 W on day 3, which imaged at 1 fps. On day 6, we installed Pi Zero 2Ws on all traps, standardizing

imaging to 1 fps. On day 6, we also extended the imaging hours from 5:00 a.m.–4:00 p.m. to 6:00 a.m.–8:00 p.m. to increase daylight coverage. Imaging at 1 fps for 14 h/day, data storage and battery power lasted ~72 h. We captured images at 2304 × 1296 pixels with the focal plane set just above the platform (Figure 1B). Camera trap software is available at https://github.com/warren-lab/bee_cam_basic.

2.2 | Platform Variants

We developed five platform variants: green, yellow, blue, fluorescent blue, and a bullseye pattern. Platforms were 35.6 cm × 20.3 cm rectangles of white corrugated plastic, printed with color ink. To make a clear coat that fluoresced blue in ultraviolet light, we dissolved Risk Reactor Clear Blue Fluorescent Solvent Based Dye (Risk Reactor, Santa Ana, CA, USA) in methyl ethyl ketone, mixing the solution into clear nail polish (Sally Hansen Xtreme Wear, Invisible; Denton, TX, USA). The two fluorescent blue platforms were standard blue platforms coated with this solution. Green, yellow, and blue colors were used in prior studies (Acharya et al. 2021; Cane et al. 2000; Ostroverkhova et al. 2018). The bullseye platform had a green background with an array of blue rings (Figure 1C; 2.7 cm diameter) painted with fluorescent clear coat around yellow circles (Figure 1C; 1.5 cm diameter). The constituent colors in the bullseye platform matched those in single-color platforms. We chose a repeating pattern because patches of colored circles are more detectable by bees than solitary disks (Wertlen et al. 2008). We reapplied the fluorescent clear coat to the fluorescent blue and bullseye platforms twice in 18 days.

2.3 | Spectroscopy

We measured reflectance of the platform variants in the 350–1000 nm range with an Ocean Optics Spectrometer using a white lamp with tungsten filament (Ocean Optics, Orlando, FL, USA). We normalized sample reflectance by subtracting the background and measured photoluminescence (PL) of our fluorescent clear coat using an Ocean Optics USB2000-FLG Spectrometer (405 nm laser excitation with 410 nm long-pass filter). We averaged PL spectra from three locations on each sample and corrected for detector sensitivity using the AM1.5 Direct Solar reference (PV Education). Nail polish alone showed no PL under 405 nm excitation. We measured PL decay of the fluorescent clear coat by positioning a sample platform 2.5 cm under a UV lamp with emission recorded every 1–2 days, then weekly until stable. We estimated field-equivalent exposure by comparing the integrated UV energy (300–400 nm) of the AM1.5 solar spectrum with the UV lamp, yielding a conversion ratio from lamp time to field-exposure days. Normalized fluorescence intensity declined to 31.7% of its initial value after eight exposure days and to 13.4% after ~57 days. We modeled fluorescence decay as $\mathrm{PL}(t) = \mathrm{a}e^{-\mathrm{k}t} + \mathrm{c}$, where t is exposure time in days. Fitting this model to the normalized data yielded a decay constant of $k = 0.254\ \mathrm{day}^{-1}$. We compared blue platform reflectance and clear-coat fluorescence to published blue vane trap spectra by independently normalizing the 400–600 nm ranges and assessing relative peak positions and spectral shape (Ostroverkhova et al. 2018).

2.4 | Sampling Protocol

We deployed the 10 camera traps in a red clover (*Trifolium pratense*) seed field at Hyslop Field Research Laboratory (Oregon State University, Corvallis, OR) during peak bloom (July 11–29, 2024). Red clover is highly attractive to bumble bees, as documented at this location and nearby sites (Anderson et al. 2010; Rao and Stephen 2009; Rao and Stephen 2010). We randomly assigned platform locations to trap types and re-randomized them on 18 and 23 July, respectively. We excluded 17 July as a sampling day because all cameras were inactive on that date due to power loss. From 25 July to 2 August, we deployed blue vane traps along the field edge ~200 m east of the cameras. We emptied the blue vane traps, which had clear jars without liquid, every ~48 h; we then froze, pinned, and identified specimens. We conducted hand-netting on 15 July with one observer and on 1 August with four observers. Following established protocol (Krahner et al. 2021), observers walked transects in clover plots for 10 min, collecting any bees within 1 m width. Bees were euthanized with ethyl acetate, pinned, and identified by OSU expert taxonomists.

2.5 | Insect Detection Model Development

We developed insect detection models using a workstation computer (Ubuntu 22.04) with a single A4500 GPU (Nvidia, Santa Clara, CA, USA). We built a dataset of annotated images using LabelImg (1.8.6; Tzutalin 2015) to manually draw bounding boxes, which delimit target objects, around any distinguishable insects. We kept bounding boxes aligned with the image axes without rotating to tightly fit insect shapes. This initial dataset included both annotated images from prior fieldwork using the same camera trap platform and background images (without insects) to reduce false positives. We split the training and validation set (72.3%/27.7%) according to a date boundary, which ensured that adjacent or similar images (i.e., from the same day) were in different datasets. For all training, we fine-tuned the pretrained You-Only-Look-Once (YOLO11s) network, which balances accuracy and computational effort according to Ultralytics benchmarks (Jocher and Qiu 2024; Redmon et al. 2016).

We compared the detection performance of two model variants: a whole-image version, which ran inference on the entire image in a single pass, and a tiling model, which operated sequentially on image subsets until the full frame was covered. For the whole-image approach, we resized images for training, validation, and inference to fit within 1280 × 1280 px while maintaining aspect. We chose this size to preserve details of small insects while enabling a batch size of 24. Batch size is the number of images loaded into GPU memory for each training iteration; larger batch sizes can improve computational efficiency and help stabilize convergence (Peng et al. 2018). To improve model generalizability, we applied augmentations during training, including flipping, scaling, and mosaic, which generates composites from the corners of four random images (Supporting Information; Shorten and Khoshgoftaar 2019). We ran this initial model on the full camera trap dataset and reviewed detections to find images containing bumble bees. We then trained a final model that included newly detected bumble bee images,

split across the training and validation sets using a date boundary (83.3% of new images, training; 16.7%, validation). We duplicated early false positives (background areas misclassified as insects) and false negatives (missed insects) to improve discrimination. The final training set included 3103 annotated images and 3232 backgrounds; the validation set contained 296 bumble bee-only images. Rather than withholding annotated data for a dedicated test set, we prioritized maximizing the size of training and validation sets.

To create the tiling training dataset, we split full images into 640 ×640 px tiles with 20% overlap. When bounding boxes were split across tiles, we retained only the tile with the largest bounding box to avoid annotation duplication and exclude small insect fragments. We pruned redundant background tiles using image hashing, which assigns each image a numeric signature based on its visual content. Tiles with highly similar hashes were treated as near-duplicates and removed. The tiled training set contained 6162 images with full or partial insects and 57,095 empty tiles; the validation set had 633 bumble bee tiles and 2436 empty tiles. Training parameters other than image size were identical to whole-image training.

We applied the trained models to all camera trap images on the Oregon State High Performance Computing cluster using a node with eight Nvidia GeForce GTX 1080 GPUs (Nvidia, Santa Clara, CA, USA). For the tiling model, we used Slicing Aided Hyper-Inference (SAHI; Akyon et al. 2022) to perform detection; as in training, a 640 ×640 px window moved stepwise across full-resolution images, with overlap to ensure full coverage. The SAHI process merges adjacent tile predictions by combining conjoined bounding boxes and removes redundant detections with non-maximum suppression, reporting detections relative to the original, full-scale image. We generated predictions for both the whole-image and tiled models using the default confidence of 0.25, which is the model's score for how likely the bounding box contains an object. Lowering this threshold would increase sensitivity; raising it would increase the likelihood of false positives.

We evaluated training performance on the bumble bee-only validation set using recall and F1 score. True positives are defined as predicted bounding boxes that overlap with the ground truth annotation by 0.5 or more. Recall is the ratio of correct detections to actual objects in the dataset; precision is the ratio of correct to total detections; F1 score is the harmonic mean of recall and precision (Pedregosa et al. 2011). We prioritized recall to minimize false negatives at the cost of including false positives, which were removed during manual review. We then evaluated the utility of both models based on their ability to detect bumble bees in unseen camera trap data.

We also compared the false positive output of both models by manually reviewing predictions sampling day 8, when all cameras acquired data for the full day. For this false positive comparison, we cropped images to the platform boundaries to reduce the visual noise of backgrounds beyond the edge. We counted any noninsect detection as a false positive. Finally, we compared model bumble bee detections to a human baseline by having a trained reviewer identify bumble bees in all images from a random day, presented as a 30-fps video.

2.6 | Diversity Estimation and Sampling Completeness

We quantified species diversity and sampling completeness using Hill numbers and sample-coverage-based rarefaction and extrapolation, using the R package *iNEXT* (Chao et al. 2014; Hsieh et al. 2016). Hill numbers unify classic diversity metrics by converting richness (q_0, the count of species present), Shannon diversity (q_1, which incorporates both richness and evenness of relative abundances), and Simpson diversity (q_2, which emphasizes the dominance of common species) into "effective number of species," placing these indices on a common, continuous scale ($q \geq 0$). *iNEXT* generates standardized rarefaction and extrapolation curves, which estimate expected diversity at various sample sizes, with an asymptotic diversity estimate corresponding to infinite sampling. We assessed sampling completeness using coverage, the proportion of total community abundance represented by individuals sampled (Chao et al. 2014). Coverage-based rarefaction/extrapolation allows comparison across methods at equivalent completeness levels, regardless of differences in sample size (Chao et al. 2014).

2.7 | Modeling and Statistical Tests

We used a permutation test to assess whether the observed visit counts to distinct platforms differed from a null model of random visitation. We randomly reassigned visits to traps, counting the visits only if the assigned camera was active. We then compared the observed counts to the distributions obtained via random permutation. We ran 10,000 iterations and adjusted *p*-values for multiple comparisons using the false discovery rate. To quantify the effect of adding fluorescence, we compared the simulated distribution of differences between fluorescent blue and blue platform visit counts to the observed difference.

To address variation in camera frame rate across the study period (0.5 fps for eight cameras during the first week, 1 fps for two cameras during the first week and for all cameras thereafter), we performed a sensitivity analysis in which all observations captured at 1 fps were subsampled to a 0.5 fps equivalent. We reran the visitation permutation test, randomly dropping 50% of single-frame visits recorded by 1 fps cameras for each iteration to simulate the reduced detection probability. Both the observed counts and simulated null distributions were subsampled for fair comparison.

To test whether camera trap location influenced visitation rates independently of platform type, we performed a blocked permutation test. For each of 10,000 iterations, each observed visit was randomly assigned to one of the two cameras with the same platform type within the same randomization block, again counted only if the assigned camera was on at the visit time. We measured aggregate effects with a chi-squared statistic (the sum of squared deviations between observed and expected counts across all 10 platforms, divided by expected counts) and per-platform, two-sided *p*-values based on absolute deviation from the simulated median. Per-platform *p*-values were corrected for multiple comparisons using the false discovery rate.

We modeled camera trap sampling efficiency for low- and high-diversity communities using two datasets: abundance data from all camera traps in this study (six species), and Oregon Bee Atlas observations (13 species) from an 18 × 12 km area in and around Bend, OR (Best 2026). The latter observations were specimen records obtained from netting surveys or blue vane traps. For each dataset, we estimated mean sample coverage by bootstrapping species abundance data for 1, 2, and 3 cameras across 25 days, with 95% confidence intervals. We calculated coverage in Python using a function adapted from *PyNext* (https://github.com/davidlevybooth/pynext). We fit the observed data from this study to a negative binomial distribution, which we used to randomly simulate hourly detections for a 14-h sampling period.

2.8 | Software

We conducted analysis and visualization in Python (3.12.0) using packages *pandas* (2.1.1), *Matplotlib* (3.8.0), *Numpy* (1.26.1), *Seaborn* (0.13.0), *Scipy* (1.11.3), and *statsmodels* (Hunter 2007; Seabold and Perktold 2010; Virtanen et al. 2020; Waskom 2021). Code is available at https://github.com/warren-lab/bee_cam_analysis.

3 | Results

3.1 | Image Collection

Over 18 days, our custom-built camera traps collected 5.7 million images (Figure 1A,B). Our platform lures included three solid colors (blue, yellow, and green), a blue platform with a fluorescent clear coat, and a high-contrast platform that mimicked floral bullseye cues (Figure 1C). As we intended, the peak reflectance (~430 nm) of the blue platform matched blue vane traps (Figure 1D) and aligned with bee photoreceptor sensitivity (Briscoe and Chittka 2001; Ostroverkhova et al. 2018; Peitsch et al. 1992). The blue vane trap reflectance, however, was much more narrowly distributed around the peak, indicating higher spectral purity. The green and yellow platforms both had peak reflectance at ~520 nm, though the yellow reflected strongly at wavelengths up to 600 nm. The photoluminescence of the fluorescent clear coat closely matched the blue vane trap, with a narrow peak at 430 nm (Figure 1E).

We compared the efficacy of using a whole image object detection model (Figure 2A) and an alternative tiling approach, which detected insects within overlapping subframes and aggregated predictions (Figure 2B,C). The tiling model exhibited

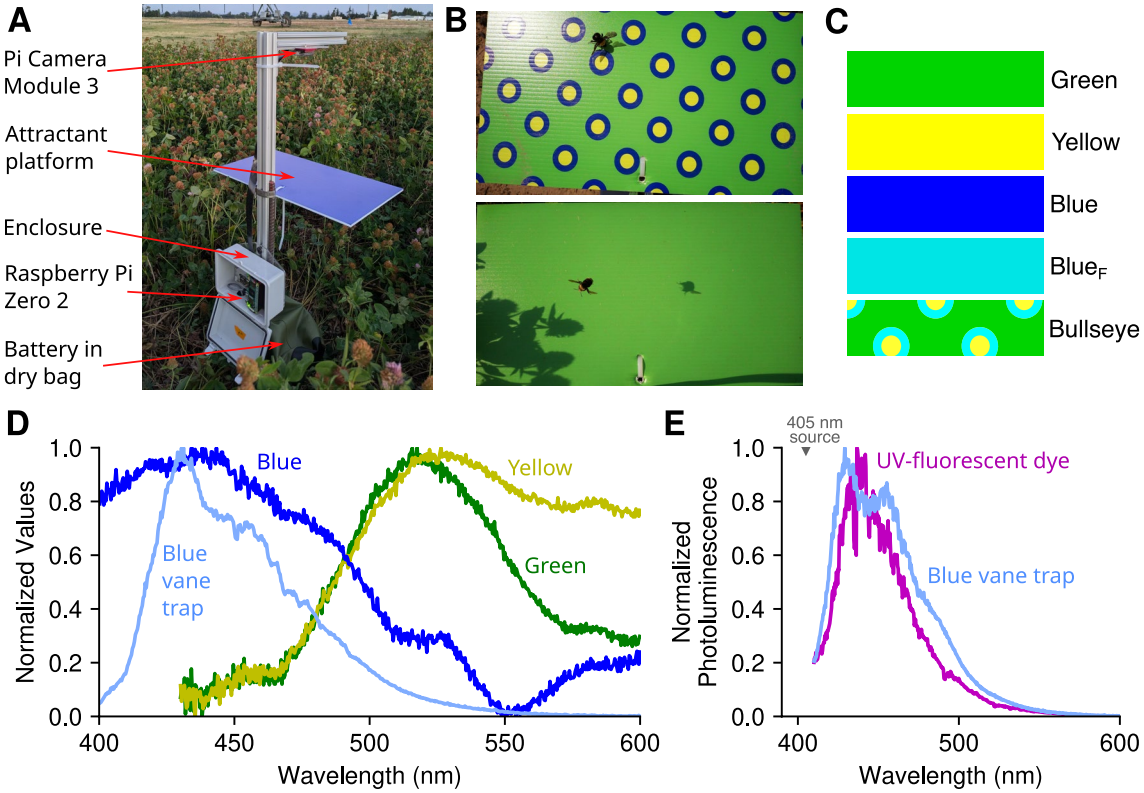

FIGURE 1 | Design of an automated insect camera trap with non-rewarding attractant platforms. (A) The custom-built camera trap was battery powered and controlled by a Raspberry Pi microcomputer. The camera was directed downward toward a platform with a printed color or pattern. (B) Example images captured by a camera trap. (C) We used five platform variants: Blue, green, yellow, blue with fluorescent clear coat paint (Blue$_F$), and a repeating bullseye pattern made up of green, yellow, and blue with fluorescence. (D) Normalized reflectance spectra of the platform colors and a blue vane trap. The blue platform reflectance spectrum peaked near 430 nm, but was broader compared to the blue vane trap. The green platform spectrum has a constrained peak, whereas the yellow platform was broader, spanning 500–600 nm. (E) Normalized photoluminescence (PL) spectrum of the blue-fluorescent dye used in our clear coat paint under 405 nm laser excitation. The fluorescent dye PL spectrum closely matches that of the blue vane trap.

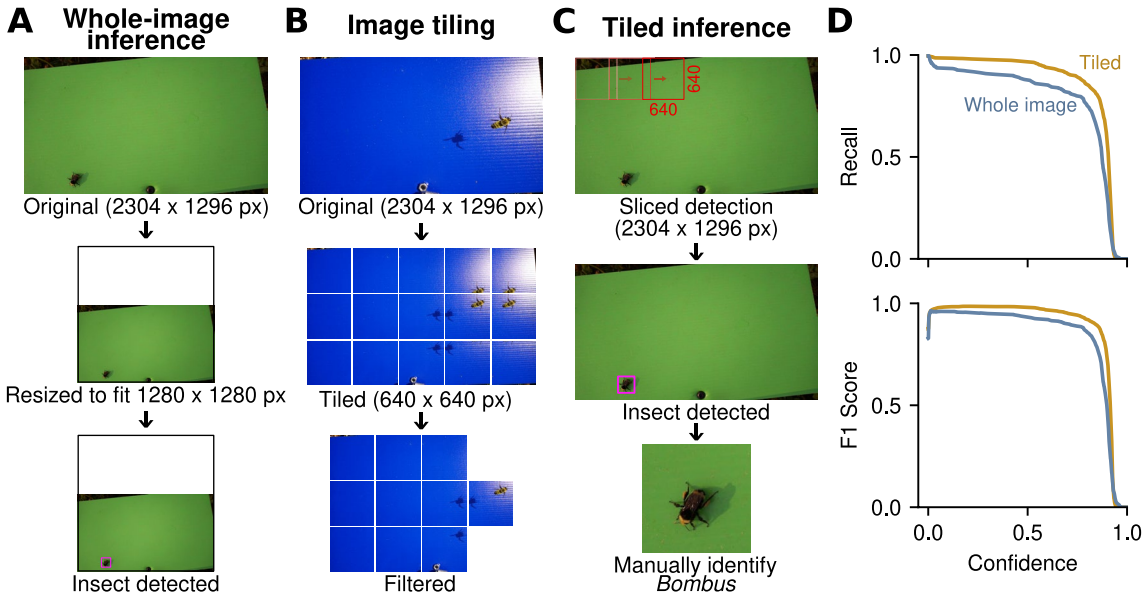

FIGURE 2 | A tiling approach outperformed a whole-image insect detection model. (A) For whole-image detection models, the original 2304 × 1296 px image was resized to 1280 × 1280 px, which we used for inference. (B) For tiling models, we divided the original image into overlapping 640 × 640 px segments and filtered to removed partial insect fragments. (C) We used Slicing-Aided Hyper Inference (SAHI) for insect detection, which processed overlapping 640 × 640 px frames across the entire image and then aggregated the predictions. From the detected insects, we manually identified bumble bees. (D) Recall-confidence and F1-confidence plots comparing the tiled (gold) and whole-image (blue-gray) models trained from YOLO11s weights. Recall measures the proportion of true positives correctly identified across confidence thresholds. The F1 score is the harmonic mean of recall and precision (the proportion of positive determinations that are correct), providing a balanced measure of model performance that penalizes both false positives and negatives. The tiling model detected 76.3% more bumble bee images in new camera trap data than the whole-image model.

better performance on a validation set of 296 images containing bumble bees, with higher recall and F1 scores across nearly all confidence thresholds (Figure 2D). At a confidence level of 0.5, the tiling model achieved 96.8% recall and 98.1% F1, compared to 87.8% recall and 93.3% F1 for the whole-image model. When applied to camera trap data outside of the training and validation set, the tiling model detected bumble bees in 76.3% more images (4894 vs. 2776) without missing any found by the whole-image model. The tiling model also produced fewer false positive detections of insects; from a single day of 495,441 images, the mean ratio across all traps of false to true positives was 0.014 and 0.036 for the tiling and whole-image models, respectively. Furthermore, the tiling model outperformed a human reviewer, detecting 20% more images with bumble bees from a randomly chosen test day. However, the tiling approach was considerably slower, averaging 1.1 images per second compared with 88.5 images per second for the whole-image model.

3.2 | Bumble Bee Visits to Platform Types

Our tiling model detected 7670 bumble bee images across the five platform types over 18 days. Daily counts (Figure 3A, top) varied independently of the amount of time cameras were operating each day (Figure 3A, bottom). Camera runtime for each platform type ranged from 342.5 to 419.2 h (blue and yellow platforms, respectively). To identify unique bee visits, we established a time-gap threshold by considering intervals between consecutive detections of the same *Bombus* species (c.f. Sittinger et al. 2024). We found that 93.8% of same-species, consecutive images occurred within 4 s, with none between 4 and 10 s (Figure 3B). Therefore, we grouped same-species detections within 4 s, yielding 291 putative unique bumble bee visits. In only two cases were multiple bumble bees present on the trap simultaneously; we manually adjusted records to include each individual. Across all traps, visitation frequency peaked between 9:00 and 10:00 a.m., though we recorded activity during all hours between 6:00 a.m. and 8:00 p.m. (Figure 3C). Bullseye platforms received the most visits (95; 20.8 detections per 10 k images), followed by green (71; 14.7), fluorescent blue (54; 9.4), blue (36; 6.4), and yellow (35; 7.1; Figure 3D).

We assessed whether the observed visit counts to distinct platforms differed from a null model of random visitation. To do this, we assigned all observed bumble bee visits to a random platform 10,000 times—counting visits only if the associated camera was recording. Observed visit counts to the bullseye and green platforms were significantly higher than this permuted distribution (bullseye, $p < 0.001$; green, $p = 0.015$; Figure 3E). The fluorescent blue and blue platforms were not significantly different from the permuted distribution, and the yellow count was significantly lower ($p = 0.004$; Figure 3E). After controlling for multiple comparisons, visit counts to bullseye and green platforms remained significantly higher than chance ($p < 0.001$, $p = 0.025$, respectively), whereas yellow platforms stayed lower ($p = 0.01$). We used these randomly permuted data to test whether adding a fluorescent clear coat increased bumble bee visitation. The observed difference in visits between the fluorescent and blue platforms (18) had a p-value of 0.058, suggesting any attractive effect of the fluorescent coat was modest. To assess whether changes in camera capture rate affected our results, we repeated this permutation test after randomly subsampling half of all single-frame

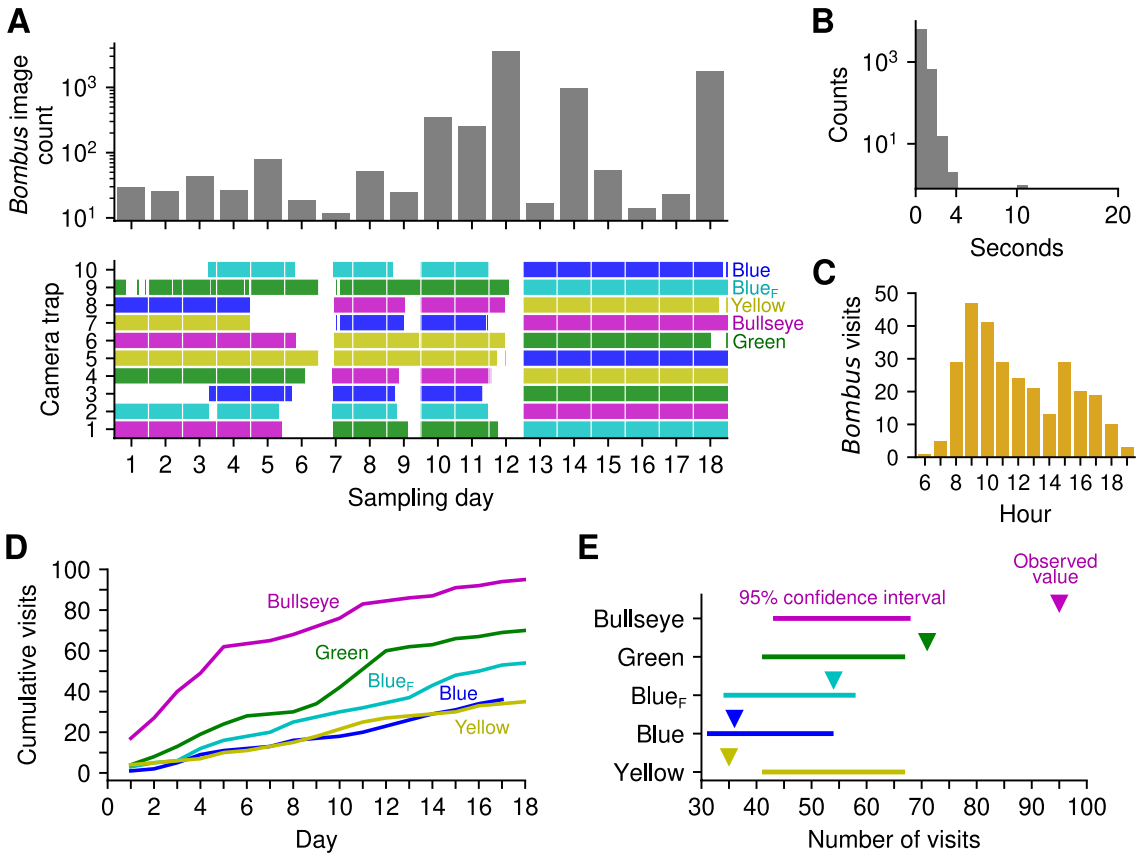

FIGURE 3 | *Bombus* visitation across platform types. (A) Daily counts of images containing bumble bees (top), with platform type and camera on-times (shaded segments) during each day's sampling period (bottom). Across all panels, BlueF refers to platforms with blue ink with a fluorescent clear coat. (B) Distribution of time intervals between consecutive images of the same bumble bee species. We used a 4 s threshold to define a unique visit; 93.8% of intervals were shorter than 4 s; none fell between 4 and 10 s. (C) Distribution of bumble bee visits by time of day from 6:00 a.m. to 7:00 p.m. (D) Cumulative bumble bee visit counts across platform types. (E) Distributions of permutation test results from 10,000 iterations in which bumble bee visit times were randomly assigned to traps and counted if the corresponding camera was on at that time. Simulated visit counts were normally distributed for each platform type; horizontal lines indicate the 95% confidence interval and triangles mark observed visit counts.

visits recorded by 1 fps cameras. The results were qualitatively unchanged; bullseye ($p < 0.001$) and green ($p = 0.006$) remained significantly higher than expected, and yellow ($p = 0.03$) was significantly lower. Single-frame visits made up 92.2% of the original detections, emphasizing the importance of a frame rate ≥ 1 fps. We found no significant effect of location on visitation rates, either in aggregate ($\chi^2 = 4.03$, $p = 0.59$) or for any individual site. We additionally observed no relationship between reapplication of fluorescent paint and visitation frequency. These findings suggest that the bullseye pattern was more attractive than any of its constituent colors, whereas camera trap location did not significantly affect visitation.

Expert taxonomists manually identified bumble bees to species using images detected by the automated tiling model. Six distinct *Bombus* species were recorded: *B. vosnesenskii*, *B. fervidus*, *B. griseocollis*, *B. nevadensis*, *B. mixtus*, and *B. appositus* (Figure 4A). Species composition and richness varied among platform types, with single visits of infrequent species driving differences (Figure 4B). The two most common species, *B. vosnesenskii* and *B. fervidus*, were most frequently observed at all five platform types. Based on prior surveys, a small percentage (2%–3%) of bees identified as *B. vosnesenskii* were likely *B. caliginosus*; the two species are difficult to distinguish using images or field observation (Rao and Stephen 2009). Thirty bumble bee images were not identified to species. Green and yellow platforms were primarily visited by *B. vosnesenskii* and *B. fervidus*. *B. griseocollis*, the third most common species, was recorded on bullseye, blue, and fluorescent blue platforms. The highest species richness, of five, was recorded by the bullseye and fluorescent blue platforms—which captured *B. nevadensis*, *B. mixtus* (bullseye platform only), and *B. appositus* (fluorescent platform only).

3.3 | Comparison of Sampling Methods

We evaluated capture rates from overlapping sampling with blue vane traps, hand netting, and cameras. Over eight consecutive days (five of which overlapped with camera sampling), two blue vane traps collected 449 insects, including 130 bumble bees. Two sessions of hand netting collected 176 bumble bees and 13 non-*Bombus* bees. Blue vane traps captured the highest bumble bee species richness, followed by camera traps and hand netting (seven, six, and five, respectively). The most common bee, *B. vosnesenskii*, was collected 3.94 times per day with blue vane traps and 0.96 times per day on camera traps (Figure 5A). On average, the blue vane traps captured 7.8 bumble bees per trap

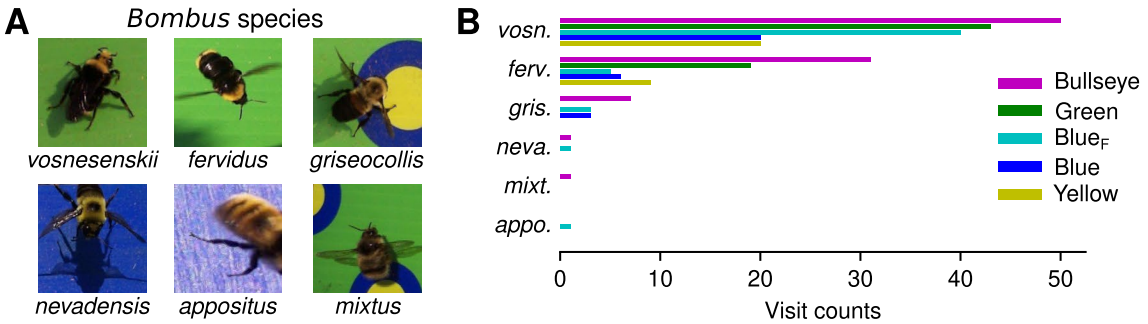

FIGURE 4 | *Bombus* species visitation by platform. (A) Cropped examples for each species of bumble bees detected on camera traps. (B) Distribution of bumble bee species visits across platform types (Blue$_F$ = blue with fluorescent clear coat).

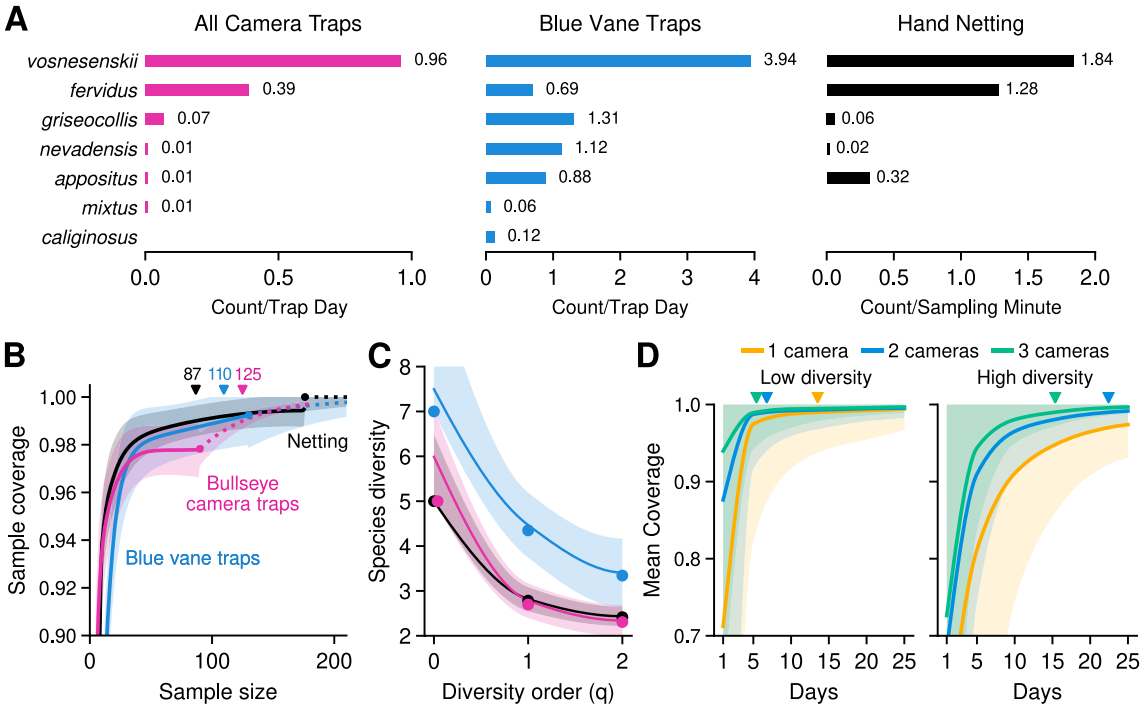

FIGURE 5 | Comparison of capture rates, diversity estimates, and coverage across sampling methods. (A) Capture rate per species for all 10 camera traps, two blue vane traps, and 50 min of netting. Camera and blue vane trap rates were standardized as individuals per trap per day; netting was standardized as individuals per sampling minute. (B) Sample coverage (the estimated proportion of individuals in the community represented by observed species) as a function of sample size for each method for blue vane traps (blue), netting (black), and two camera traps with bullseye platforms (pink). Solid lines show rarefaction; dotted lines show extrapolation; circle markers are observed values; shaded regions are 95% confidence intervals (CI). The small gap between the netting rarefaction and extrapolation curves reflects reduced coverage caused by downsampling in rarefaction. Triangles indicate the sample count at which each method reaches 0.99 coverage. Statistics were computed with *iNEXT*. (C) Asymptotic diversity estimates across Hill numbers (q_0 = richness, q_1 = Shannon diversity, q_2 = Simpson diversity) for each method; colors are the same as panel B. Asymptotic estimates predict the diversity expected with complete sampling. Circles mark observed values; solid lines show estimated values; shaded regions are 95% CI. (D) Bootstrapped estimates of sample coverage over time for different numbers of camera traps at a low-diversity site (6 species; current study) and a high-diversity site (13 species; Oregon Bee Atlas data from Bend, OR). Rate of capture is modeled using the observed visitation rate to the bullseye platform. Shaded regions represent the 95% CI for each camera number; the upper bound of each CI is 1.0. Triangles mark when 0.99 coverage is reached.

daily, whereas hand netting yielded 3.5 bumble bees per person per 10-min session (Figure 5A). The camera traps together averaged 2.1 visits per sample day, whereas the bullseye platforms averaged 3.3 visits per day.

We compared the efficiency of sampling methods by determining how coverage (the estimated proportion of individuals in the community represented by all observed species) varied with sample size. Netting was the most efficient sampling method at reaching 0.99 coverage, followed by blue vane traps and cameras (87, 110, and 125 samples, respectively; Figure 5B). We compared asymptotic diversity estimates across sampling methods to account for unequal effort. The blue vane traps outperformed the other methods across diversity orders, yielding the highest estimated richness, $q_0 = 7.5$ (95% CI: 7.0–10.3), evenness, $q_1 = 4.5$ (3.8–5.2), and diversity,

$q_2 = 3.4$ (2.7–4.1; Figure 5C). Diversity estimates for netting ($q_0 = 5.0$, 95% CI: 5.0–6.3; $q_1 = 2.8$, 2.5–3.1; $q_2 = 2.4$, 2.2–2.7) and the two camera traps ($q_0 = 6.0$, 95% CI: 5.2–6.8; $q_1 = 2.8$, 2.4–3.2; $q_2 = 2.3$, 2.0–2.7) mostly overlapped, suggesting comparable performance. The higher richness estimate for the cameras suggests that additional species would likely be detected with increased sampling effort.

We simulated how camera-based sampling scales with effort using a bootstrapping approach to estimate coverage with varying numbers of camera traps and levels of bumble bee diversity. To model a low-diversity site, we used the species abundance distribution from all camera traps in this study (six species). We found that one camera reached 0.99 coverage after 13.5 days, whereas two and three cameras took 6.8 and 5.4 days, respectively (Figure 5D, left). To model a high diversity site, we used data previously collected near Bend, OR, which included 13 species (Figure 5D, right). For this site, two cameras reached 0.99 coverage in 22.4 days, whereas three took 15.4 days. One camera reached a maximum of 0.97 coverage after 25 days. These results suggest that deploying multiple cameras substantially accelerates reaching sampling completeness, especially at high-diversity sites.

4 | Discussion

In this study, we developed and tested a custom, low-cost camera trap for continuous, nonlethal monitoring of diurnal insect pollinators. We found that a tiling approach (Figure 2B,C) markedly improved automated insect detection and bumble bee recall (Figure 2D). Bumble bee visitation was highest on platforms with a fluorescent bullseye pattern (Figure 3E). In total, camera traps recorded six bumble bee species, which closely matched netting and blue vane traps (Figure 5B). Through simulations, we predict that deploying additional cameras will yield substantial gains in sampling completeness at species-rich sites, with diminishing returns at low-diversity locations (Figure 5D). Our results show that camera traps can provide community-level assessments comparable to conventional lethal sampling. The work provides a foundation for the development of scalable, non-invasive long-term monitoring of vulnerable bee populations.

Our camera trap monitoring was semi-automated. We collected data continuously via time-lapse imaging and then detected insects offline with custom-built deep learning models. Expert human taxonomists identified bumble bees to species. A key finding of this study is that Slicing Aided Hyper-Inference (SAHI), which partitions source images into overlapping tiles, markedly improved insect detection. Indeed, tiled models identified 76% more images with bumble bees than whole-image models, with fewer false positives. Tiling has been shown to improve detection of small objects (i.e., object width $<1\%$ of image width) in other datasets such as satellite photos (Akyon et al. 2022; Svenning et al. 2026). Few studies, however, have previously examined tiling in insect detection (Svenning et al. 2026; Ye et al. 2024). Tiling likely improves small-object detection primarily by increasing effective resolution, dedicating more pixels to each object. Additionally, by increasing the relative size in the frame of the targets to be detected, tiling better matches the large objects used in datasets to pretrain YOLO models (Akyon et al. 2022).

Our findings could help guide further automation of camera systems. Recent studies developed real-time insect detection models, with reduced neural network size and image resolution (Bjerge et al. 2022; Sittinger et al. 2024). These models can enable immediate culling of empty images, thereby reducing on-device storage and downstream processing. A potential issue, however, with real-time detection is the additional power consumption of AI inference, which could restrict data collection to limited time windows within the day (Künast et al. 2026; Sittinger et al. 2024). We found that bumble bees visited platform lures throughout all daylight hours (Figure 3C). Therefore, full characterization of bumble bee communities, with sensitivity to rare species, may require full-day monitoring. An additional concern with real-time detection is the potential for false negatives, which could result in inadvertent data loss. Future monitoring could take a hybrid approach—with permissive, online detection models for initial data filtering, followed by offline tiling approaches for precise, reliable insect localization.

Beyond the initial detection of insects on image frames, another key challenge is automating species identification. We found that dorsal camera trap images were sufficiently detailed to enable species-level classification by expert human taxonomists. A recent study used a deep-learning classifier to perform species-level identification from camera trap images (Sittinger et al. 2024; Spiesman et al. 2021). However, the extent to which trained classification models generalize across camera trap systems is not well understood. Cryptic species (e.g., *B. vosnesenskii* and *B. caliginosus*) and region-specific variants may challenge species-level classification (Ghisbain et al. 2020; Lozier et al. 2016). Additional data inputs such as acoustics (Ferreira et al. 2025; Gradišek et al. 2017; Kohlberg et al. 2024) or eDNA (De Jager et al. 2017; Jones et al. 2025; Pilliod et al. 2025) may improve taxonomic fidelity.

Our results suggest that a repeating bullseye pattern, mimicking floral contrast cues, could be broadly useful as a nonlethal lure for bumble bee camera traps. Significantly more bumble bees visited bullseye platforms than those with the uniform constituent colors. This is consistent with prior observations that bullseye patterns on flowers (Horth et al. 2014; Koski and Ashman 2014) and high-contrast platforms (De Jager et al. 2017; Lunau et al. 2025) attract bees. Of the constituent colors in the bullseye pattern, the solid green platform was the most visited (Figure 3E). This differed from prior studies, in which blue platforms were most attractive (Acharya et al. 2021; Ostroverkhova et al. 2018; Sipolski et al. 2019). The lower spectral purity of our blue platforms, in comparison with blue vane traps, may have weakened their attractiveness (Figure 1D, Lunau and Dyer 2024). Green contrast cues are known to play a role in long-distance spatial processing (Chittka and Tautz 2003; Giurfa et al. 1996). The large green background and high-contrast concentric circles of the bullseye platform potentially integrate long and short-range cues; together, they may have elicited bumble bee approaches. Our study did not address the relative attractiveness and necessity of the bullseye pattern's distinct features—such as color combinations, fluorescence, and spatial orientation. It is therefore unclear whether the blue fluorescent ring in the bullseye pattern is important to its attractiveness. This could be studied further in future experiments with camera traps. Blue fluorescence is essential to the attractiveness of blue vane traps (Ostroverkhova et al. 2018); however,

we observed only a modest effect of adding a fluorescent coat to a solid blue platform. This could be due in part to the low spectral purity of the blue ink (Figure 1D). In summary, the high bumble bee recruitment to bullseye platforms and blue vane traps indicates the attractiveness of contrast patterns and spectrally pure fluorescent colors.

Our camera trap sampling estimates of a specific bumble bee community closely matched the results of two conventional methods conducted concurrently. Lethal sampling with blue vane traps collected the largest numbers of bumble bees, with the highest estimated species richness and diversity (Figure 5B; Hall 2018; Kimoto et al. 2012; Stephen and Rao 2005). Hand netting achieved full sample coverage with the fewest specimens but yielded the lowest richness (Figure 5B,C). This is consistent with prior studies suggesting that rare species can remain undetected even when sampling is estimated as complete (Benoit et al. 2018; Fisher et al. 2022; Sgarbi et al. 2020). Active netting allows targeted, rapid accumulation of specimens; however, it is constrained by observer skill, weather, and limited temporal coverage. This can result in biased detection of species that are abundant, easily captured, or differentially active at particular times of day (O'Connor et al. 2019; Popic et al. 2013). The two most attractive camera traps, with bullseye platforms, matched netting in observed species richness despite capturing fewer specimens. These two camera traps also yielded higher estimated richness than netting (six vs. five). One caveat is that our coverage and estimated richness calculations assume all observed bees are distinct individuals; lethal collection with netting or blue vane traps guarantees this condition, whereas passive cameras may record the same individual multiple times. Any double-counting of individuals would result in overestimates of coverage and estimated richness. Future studies could use mark-and-recapture experiments to directly measure revisitation rate to camera traps. Our simulations showed that increasing the number of cameras may substantially improve sampling efficiency, particularly at high-diversity sites (Figure 5D). The scalability of camera traps may therefore be crucial for detecting rare species, which can require extensive sampling in diverse areas (Fisher et al. 2022).

With refinement of visual lures and detection algorithms, camera traps could offer a robust, noninvasive alternative to traditional lethal methods. Unlike netting, camera traps operate continuously, are noninvasive, and can be deployed at scale; unlike vane traps, image-based sampling is nonlethal and provides precise visit times that can be leveraged for analysis of species-specific activity patterns. Distributing a network of camera traps across a landscape could fill gaps in the data patchwork of species presence, climate niche occupancy, and community associations, providing a more comprehensive view of pollinator health and ecology. Continuous, spatially extensive monitoring of bees would improve detection of rare and endangered species, help link insect activity with environmental variables, and enable mark-and-recapture experiments that monitor foraging distances and population dynamics.

Author Contributions

Michael P. Getz: conceptualization, investigation, writing – original draft, writing – review and editing, data curation, formal analysis, software, methodology, validation, visualization. **Lincoln R. Best:** conceptualization, investigation, methodology, writing – review and editing. **Oksana Ostroverkhova:** investigation, methodology, writing – review and editing, supervision. **Andony P. Melathopoulos:** conceptualization, investigation, writing – review and editing, methodology, supervision. **Timothy L. Warren:** conceptualization, investigation, funding acquisition, methodology, writing – review and editing, project administration, supervision, resources, data curation.

Acknowledgments

We thank Madalyn Gragg and Jason Culley for collecting spectral data from the platforms, and taxonomists August Jackson and Brooke Ruby for identifying specimens and insects in images. We thank Nathaniel Davidson, Liam Hodge, Logan Rower, and Konstantin Savkin for manually reviewing image data. We thank Nevin Cullen, N. Davidson, and Darren Miller for commenting on an earlier draft.

Funding

This work was supported by the California Department of Fish and Wildlife (Q2491217), the National Institute of Food and Agriculture (2020-05857), and the U.S. Department of Agriculture (58-2072-3-025).

Data Availability Statement

All software and camera trap methods are open-source. Data analysis software is https://github.com/warren-lab/bee_cam_analysis. Camera trap software is at https://github.com/warren-lab/bee_cam_basic. Annotated image data is available at a Zenodo repository: doi: 10.5281/zenodo.19870171.

References

Acharya, R. S., T. Leslie, E. Fitting, J. Burke, K. Loftin, and N. K. Joshi. 2021. "Color of Pan Trap Influences Sampling of Bees in Livestock Pasture Ecosystem." *Biology* 10: 445. https://doi.org/10.3390/biology10050445.

Akyon, F. C., S. O. Altinuc, and A. Temizel. 2022. "Slicing Aided Hyper Inference and Fine-Tuning for Small Object Detection." *2022 IEEE International Conference on Image Processing (ICIP)*: 966–970. https://doi.org/10.1109/ICIP46576.2022.9897990.

Anderson, N., P. S. Rao, and A. V. Derkatch. 2010. "Native Bumble Bee Diversity, Abundance, and Pollination in Crimson Clover and Hairy Vetch Seed Production Fields in Western Oregon." *Seed Production Research* 8.

Benoit, D., D. A. Jackson, and M. S. Ridgway. 2018. "Assessing the Impacts of Imperfect Detection on Estimates of Diversity and Community Structure Through Multispecies Occupancy Modeling." *Ecology and Evolution* 8: 4676–4684. https://doi.org/10.1002/ece3.4023.

Best, L. R. 2026. "Oregon Bee Atlas." https://doi.org/10.15468/fqxchw.

Biesmeijer, J. C., S. P. M. Roberts, M. Reemer, et al. 2006. "Parallel Declines in Pollinators and Insect-Pollinated Plants in Britain and The Netherlands." *Science* 313: 351–354. https://doi.org/10.1126/science.1127863.

Bjerge, K., J. Alison, M. Dyrmann, C. E. Frigaard, H. M. R. Mann, and T. T. Høye. 2023. "Accurate Detection and Identification of Insects From Camera Trap Images With Deep Learning." *PLOS Sustainability and Transformation* 2: e0000051. https://doi.org/10.1371/journal.pstr.0000051.

Bjerge, K., H. Karstoft, and T. T. Høye. 2025. "Towards Edge Processing of Images From Insect Camera Traps." *Remote Sensing in Ecology and Conservation* 11: 573–589. https://doi.org/10.1002/rse2.70007.

Bjerge, K., H. M. Mann, and T. T. Høye. 2022. "Real-Time Insect Tracking and Monitoring With Computer Vision and Deep Learning." *Remote Sensing in Ecology and Conservation* 8: 315–327.

Boom, B. J., J. He, S. Palazzo, et al. 2014. "A Research Tool for Long-Term and Continuous Analysis of Fish Assemblage in Coral-Reefs Using Underwater Camera Footage." *Ecological Informatics* 23: 83–97. https://doi.org/10.1016/j.ecoinf.2013.10.006.

Boyer, K. J., F. P. Fragoso, M. E. Dieterich Mabin, and J. Brunet. 2020. "Netting and Pan Traps Fail to Identify the Pollinator Guild of an Agricultural Crop." *Scientific Reports* 10: 13819. https://doi.org/10.1038/s41598-020-70518-9.

Briscoe, A. D., and L. Chittka. 2001. "The Evolution of Color Vision in Insects." *Annual Review of Entomology* 46: 471–510.

Cameron, S. A., J. D. Lozier, J. P. Strange, et al. 2011. "Patterns of Widespread Decline in North American Bumble Bees." *Proceedings of the National Academy of Sciences* 108: 662–667. https://doi.org/10.1073/pnas.1014743108.

Cameron, S. A., and B. M. Sadd. 2020. "Global Trends in Bumble Bee Health." *Annual Review of Entomology* 65: 209–232. https://doi.org/10.1146/annurev-ento-011118-111847.

Cane, J. H., R. L. Minckley, and L. J. Kervin. 2000. "Sampling Bees (Hymenoptera: Apiformes) for Pollinator Community Studies: Pitfalls of Pan-Trapping." *Journal of the Kansas Entomological Society* 73: 225–231.

Chao, A., N. J. Gotelli, T. C. Hsieh, et al. 2014. "Rarefaction and Extrapolation With Hill Numbers: A Framework for Sampling and Estimation in Species Diversity Studies." *Ecological Monographs* 84: 45–67. https://doi.org/10.1890/13-0133.1.

Chao, A., Y. Kubota, D. Zelený, et al. 2020. "Quantifying Sample Completeness and Comparing Diversities Among Assemblages." *Ecological Research* 35: 292–314. https://doi.org/10.1111/1440-1703.12102.

Chesshire, P. R., E. E. Fischer, N. J. Dowdy, et al. 2023. "Completeness Analysis for Over 3000 United States Bee Species Identifies Persistent Data Gap." *Ecography* 2023: e06584. https://doi.org/10.1111/ecog.06584.

Chittka, L., and J. Tautz. 2003. "The Spectral Input to Honeybee Visual Odometry." *Journal of Experimental Biology* 206: 2393–2397. https://doi.org/10.1242/jeb.00436.

Colgan, A. M., R. G. Hatfield, A. Dolan, W. Velman, R. E. Newton, and T. A. Graves. 2024. "Quantifying Effectiveness and Best Practices for Bumblebee Identification From Photographs." *Scientific Reports* 14: 830.

De Jager, M. L., E. Willis-Jones, S. Critchley, and B. J. Glover. 2017. "The Impact of Floral Spot and Ring Markings on Pollinator Foraging Dynamics." *Evolutionary Ecology* 31: 193–204. https://doi.org/10.1007/s10682-016-9852-5.

Droissart, V., L. Azandi, E. R. Onguene, M. Savignac, T. B. Smith, and V. Deblauwe. 2021. "PICT: A Low-Cost, Modular, Open-Source Camera Trap System to Study Plant–Insect Interactions." *Methods in Ecology and Evolution* 12: 1389–1396. https://doi.org/10.1111/2041-210X.13618.

Eeraerts, M., and I. Meeus. 2025. "Different Pollinator Sampling Methods Measure Distinct Pollinator Communities in a Mass-Flowering Crop, Which Respond Differently to the Composition of the Surrounding Landscape." *Web Ecology* 25: 47–57. https://doi.org/10.5194/we-25-47-2025.

Ferreira, A. I. S., N. F. F. da Silva, F. N. Mesquita, T. C. Rosa, S. L. Buchmann, and J. N. Mesquita-Neto. 2025. "Transformer Models Improve the Acoustic Recognition of Buzz-Pollinating Bee Species." *Ecological Informatics* 86: 103010.

Fisher, K., K. M. Watrous, N. M. Williams, L. L. Richardson, and S. H. Woodard. 2022. "A Contemporary Survey of Bumble Bee Diversity Across the State of California." *Ecology and Evolution* 12: e8505.

Ghisbain, G., J. D. Lozier, S. R. Rahman, et al. 2020. "Substantial Genetic Divergence and Lack of Recent Gene Flow Support Cryptic Speciation in a Colour Polymorphic Bumble Bee (*Bombus bifarius*) Species Complex." *Systematic Entomology* 45: 635–652. https://doi.org/10.1111/syen.12419.

Giurfa, M., M. Vorobyev, P. Kevan, and R. Menzel. 1996. "Detection of Coloured Stimuli by Honeybees: Minimum Visual Angles and Receptor Specific Contrasts." *Journal of Comparative Physiology. A, Neuroethology, Sensory, Neural, and Behavioral Physiology* 178: 699–709.

Gradišek, A., G. Slapničar, J. Šorn, M. Luštrek, M. Gams, and J. Grad. 2017. "Predicting Species Identity of Bumblebees Through Analysis of Flight Buzzing Sounds." *Bioacoustics* 26: 63–76. https://doi.org/10.1080/09524622.2016.1190946.

Graves, T. A., W. M. Janousek, S. M. Gaulke, et al. 2020. "Western Bumble Bee: Declines in the Continental United States and Range-Wide Information Gaps." *Ecosphere* 11: e03141. https://doi.org/10.1002/ecs2.3141.

Gronquist, M., A. Bezzerides, A. Attygalle, J. Meinwald, M. Eisner, and T. Eisner. 2001. "Attractive and Defensive Functions of the Ultraviolet Pigments of a Flower (*Hypericum calycinum*)." *Proceedings. National Academy of Sciences. United States of America* 98: 13745–13750. https://doi.org/10.1073/pnas.231471698.

Guldberg, L. D., and P. R. Atsatt. 1975. "Frequency of Reflection and Absorption of Ultraviolet Light in Flowering Plants." *American Midland Naturalist* 93: 35–43. https://doi.org/10.2307/2424103.

Hall, M. 2018. "Blue and Yellow Vane Traps Differ in Their Sampling Effectiveness for Wild Bees in Both Open and Wooded Habitats." *Agricultural and Forest Entomology* 20: 487–495. https://doi.org/10.1111/afe.12281.

Hempel De Ibarra, N., S. Holtze, C. Bäucker, P. Sprau, and M. Vorobyev. 2022. "The Role of Colour Patterns for the Recognition of Flowers by Bees." *Philosophical Transactions of the Royal Society B* 377: 20210284. https://doi.org/10.1098/rstb.2021.0284.

Horth, L., L. Campbell, and R. Bray. 2014. "Wild Bees Preferentially Visit *Rudbeckia* Flower Heads With Exaggerated Ultraviolet Absorbing Floral Guides." *Biology Open* 3: 221–230. https://doi.org/10.1242/bio.20146445.

Hsieh, T. C., K. H. Ma, and A. Chao. 2016. "iNEXT: An R Package for Rarefaction and Extrapolation of Species Diversity (H Ill Numbers)." *Methods in Ecology and Evolution* 7: 1451–1456. https://doi.org/10.1111/2041-210X.12613.

Hunter, J. D. 2007. "Matplotlib: A 2D Graphics Environment." *Computing in Science & Engineering* 9: 90–95.

Jacobson, M. M., E. M. Tucker, M. E. Mathiasson, and S. M. Rehan. 2018. "Decline of Bumble Bees in Northeastern North America, With Special Focus on *Bombus terricola*." *Biological Conservation* 217: 437–445. https://doi.org/10.1016/j.biocon.2017.11.026.

Jocher, G., and J. Qiu. 2024. "Ultralytics YOLO11."

Jones, K. S., D. S. Pilliod, and A. W. Aunins. 2025. "Metabarcoding Analysis of Arthropod Pollinator Diversity: A Methodological Comparison of eDNA Derived From Flowers and DNA Derived From Bulk Samples of Insects." *Molecular Ecology* 34: e70003. https://doi.org/10.1111/mec.70003.

Kimoto, C., S. J. DeBano, R. W. Thorp, S. Rao, and W. P. Stephen. 2012. "Investigating Temporal Patterns of a Native Bee Community in a Remnant North American Bunchgrass Prairie Using Blue Vane Traps." *Journal of Insect Science* 12: 1–23. https://doi.org/10.1673/031.012.10801.

Kohlberg, A. B., C. R. Myers, and L. L. Figueroa. 2024. "From Buzzes to Bytes: A Systematic Review of Automated Bioacoustics Models Used to Detect, Classify and Monitor Insects." *Journal of Applied Ecology* 61: 1199–1211. https://doi.org/10.1111/1365-2664.14630.

Koski, M. H., and T. Ashman. 2014. "Dissecting Pollinator Responses to a Ubiquitous Ultraviolet Floral Pattern in the Wild." *Functional Ecology* 28: 868–877. https://doi.org/10.1111/1365-2435.12242.

Krahner, A., J. Schmidt, M. Maixner, M. Porten, and T. Schmitt. 2021. "Evaluation of Four Different Methods for Assessing Bee Diversity as Ecological Indicators of Agro-Ecosystems." *Ecological Indicators* 125: 107573.

Künast, R., S. Jeschke, P. Mäder, and S. Meyer. 2026. "Prolonged Reduction in Grassland Arthropod Activity After Mowing Revealed by AI Camera Trap Monitoring." *Basic and Applied Ecology* 94: 1–13. https://doi.org/10.1016/j.baae.2026.04.007.

Lozier, J. D., J. M. Jackson, M. E. Dillon, and J. P. Strange. 2016. "Population Genomics of Divergence Among Extreme and Intermediate Color Forms in a Polymorphic Insect." *Ecology and Evolution* 6: 1075–1091. https://doi.org/10.1002/ece3.1928.

Lunau, K., M. G. G. Camargo, and Z.-X. Ren. 2025. "Bees, Flowers and UV." *Plant Biology Journal* 27: 948–961. https://doi.org/10.1111/plb.70050.

Lunau, K., and A. G. Dyer. 2024. "The Modelling of Flower Colour: Spectral Purity or Colour Contrast as Biologically Relevant Descriptors of Flower Colour Signals for Bees Depending Upon the Perceptual Task." *Plant Biology Journal* 26: 896–910. https://doi.org/10.1111/plb.13682.

Mathis, C. L., D. J. McNeil, M. Kammerer, J. L. Larkin, and M. J. Skvarla. 2024. "Distance Models Reveal Biases Associated With Passive Trapping Methods for Measuring Wild Bee Abundance." *Frontiers in Ecology and Evolution* 12: 1380622. https://doi.org/10.3389/fevo.2024.1380622.

McNeil, D. J., C. R. V. Otto, E. L. Moser, et al. 2019. "Distance Models as a Tool for Modelling Detection Probability and Density of Native Bumblebees." *Journal of Applied Entomology* 143: 225–235. https://doi.org/10.1111/jen.12583.

Montgomery, G. A., M. W. Belitz, R. P. Guralnick, and M. W. Tingley. 2021. "Standards and Best Practices for Monitoring and Benchmarking Insects." *Frontiers in Ecology and Evolution* 8: 579193. https://doi.org/10.3389/fevo.2020.579193.

Naqvi, Q., P. J. Wolff, B. Molano-Flores, and J. H. Sperry. 2022. "Camera Traps Are an Effective Tool for Monitoring Insect–Plant Interactions." *Ecology and Evolution* 12: e8962. https://doi.org/10.1002/ece3.8962.

O'Connor, R. S., W. E. Kunin, M. P. D. Garratt, et al. 2019. "Monitoring Insect Pollinators and Flower Visitation: The Effectiveness and Feasibility of Different Survey Methods." *Methods in Ecology and Evolution* 10: 2129–2140. https://doi.org/10.1111/2041-210X.13292.

Ostroverkhova, O., G. Galindo, C. Lande, et al. 2018. "Understanding Innate Preferences of Wild Bee Species: Responses to Wavelength-Dependent Selective Excitation of Blue and Green Photoreceptor Types." *Journal of Comparative Physiology. A* 204: 667–675. https://doi.org/10.1007/s00359-018-1269-x.

Pedregosa, F., G. Varoquaux, A. Gramfort, et al. 2011. "Scikit-Learn: Machine Learning in Python." *Journal of Machine Learning Research* 12: 2825–2830.

Peitsch, D., A. Fietz, H. Hertel, J. De Souza, D. F. Ventura, and R. Menzel. 1992. "The Spectral Input Systems of Hymenopteran Insects and Their Receptor-Based Colour Vision." *Journal of Comparative Physiology. A* 170: 23–40. https://doi.org/10.1007/bf00190398.

Peng, C., T. Xiao, Z. Li, et al. 2018. "Megdet: A Large Mini-Batch Object Detector." In: *Proceedings of the IEEE Conference on Computer Vision and Pattern Recognition*: 6181–6189.

Pilliod, D. S., M. R. Grossklaus, S. A. Kageyama, et al. 2025. "A 21st Century Butterfly Net: Using eDNA to Detect the Imperiled Dakota Skipper." *Global Ecology and Conservation* 62: e03815.

Popic, T. J., Y. C. Davila, and G. M. Wardle. 2013. "Evaluation of Common Methods for Sampling Invertebrate Pollinator Assemblages: Net Sampling Out-Perform Pan Traps." *PLoS One* 8: e66665. https://doi.org/10.1371/journal.pone.0066665.

Rao, S., and O. Ostroverkhova. 2015. "Visual Outdoor Response of Multiple Wild Bee Species: Highly Selective Stimulation of a Single Photoreceptor Type by Sunlight-Induced Fluorescence." *Journal of Comparative Physiology. A* 201: 705–716. https://doi.org/10.1007/s00359-015-0983-x.

Rao, S., and W. P. Stephen. 2009. "Bumble Bee Pollinators in Red Clover Seed Production." *Crop Science* 49: 2207–2214. https://doi.org/10.2135/cropsci2009.01.0003.

Rao, S., and W. P. Stephen. 2010. "Abundance and Diversity of Native Bumble Bees Associated with Agricultural Crops: The Willamette Valley Experience." *Psyche: A Journal of Entomology 2010*: 1–9.

Redmon, J., S. Divvala, R. Girshick, and A. Farhadi. 2016. "You Only Look Once: Unified, Real-Time Object Detection." In: *Proceedings of the IEEE Conference on Computer Vision and Pattern Recognition*: 779–788.

Rovero, F., F. Zimmermann, D. Berzi, and P. Meek. 2013. ""Which Camera Trap Type and How Many Do I Need?" A Review of Camera Features and Study Designs for a Range of Wildlife Research Applications." *Hystrix: The Italian Journal of Mammalogy* 24, no. 2: 148–156.

Rowcliffe, J. M., R. Kays, B. Kranstauber, C. Carbone, and P. A. Jansen. 2014. "Quantifying Levels of Animal Activity Using Camera Trap Data." *Methods in Ecology and Evolution* 5: 1170–1179. https://doi.org/10.1111/2041-210X.12278.

Roy, D. B., J. Alison, T. A. August, et al. 2024. "Towards a Standardized Framework for AI-Assisted, Image-Based Monitoring of Nocturnal Insects." *Philosophical Transactions of the Royal Society B* 379: 20230108. https://doi.org/10.1098/rstb.2023.0108.

Samejima, H., R. Ong, P. Lagan, and K. Kitayama. 2012. "Camera-Trapping Rates of Mammals and Birds in a Bornean Tropical Rainforest Under Sustainable Forest Management." *Forest Ecology and Management* 270: 248–256. https://doi.org/10.1016/j.foreco.2012.01.013.

Sánchez-Bayo, F., and K. A. G. Wyckhuys. 2019. "Worldwide Decline of the Entomofauna: A Review of Its Drivers." *Biological Conservation* 232: 8–27. https://doi.org/10.1016/j.biocon.2019.01.020.

Seabold, S., and J. Perktold. 2010. "Statsmodels: Econometric and Statistical Modeling With Python." *SciPy* 7: 92–96.

Sgarbi, L. F., L. M. Bini, J. Heino, et al. 2020. "Sampling Effort and Information Quality Provided by Rare and Common Species in Estimating Assemblage Structure." *Ecological Indicators* 110: 105937. https://doi.org/10.1016/j.ecolind.2019.105937.

Shorten, C., and T. M. Khoshgoftaar. 2019. "A Survey on Image Data Augmentation for Deep Learning." *Journal of Big Data* 6: 60. https://doi.org/10.1186/s40537-019-0197-0.

Sipolski, S. J., S. W. Datson, M. Reding, J. B. Oliver, and S. R. Alm. 2019. "Minimizing Bee (Hymenoptera: Apoidea) Bycatch in Japanese Beetle Traps." *Environmental Entomology* 48: 1203–1213. https://doi.org/10.1093/ee/nvz098.

Sittinger, M., J. Uhler, M. Pink, and A. Herz. 2024. "Insect Detect: An Open-Source DIY Camera Trap for Automated Insect Monitoring." *PLoS One* 19: e0295474. https://doi.org/10.1371/journal.pone.0295474.

Spiesman, B. J., C. Gratton, R. G. Hatfield, et al. 2021. "Assessing the Potential for Deep Learning and Computer Vision to Identify Bumble Bee Species From Images." *Scientific Reports* 11: 7580. https://doi.org/10.1038/s41598-021-87210-1.

Stephen, W. P., and S. Rao. 2005. "Unscented Color Traps for Non-Apis Bees (Hymenoptera: Apiformes)." *Journal of the Kansas Entomological Society* 78: 373–380.

Svenning, A., G. Mougeot, J. Alison, et al. 2026. "A General Method for Detection and Segmentation of Terrestrial Arthropods in Images." *Methods in Ecology and Evolution* 17: 727–739. https://doi.org/10.1111/2041-210x.70249.

Teixeira, A. C., J. Ribeiro, R. Morais, J. J. Sousa, and A. Cunha. 2023. "A Systematic Review on Automatic Insect Detection Using Deep Learning." *Agriculture* 13: 713. https://doi.org/10.3390/agriculture13030713.

Tzutalin. 2015. "LabelImg." https://github.com/tzutalin/labelImg.

Van Der Kooi, C. J., A. G. Dyer, P. G. Kevan, and K. Lunau. 2019. "Functional Significance of the Optical Properties of Flowers for Visual Signalling." *Annals of Botany* 123: 263–276. https://doi.org/10.1093/aob/mcy119.

Van Der Sluijs, J. P. 2020. "Insect Decline, an Emerging Global Environmental Risk." *Current Opinion in Environmental Sustainability* 46: 39–42. https://doi.org/10.1016/j.cosust.2020.08.012.

Virtanen, P., R. Gommers, T. E. Oliphant, et al. 2020. "SciPy 1.0: Fundamental Algorithms for Scientific Computing in Python." *Nature Methods* 17: 261–272.

Wagner, D. L. 2020. "Insect Declines in the Anthropocene." *Annual Review of Entomology* 65: 457–480. https://doi.org/10.1146/annurev-ento-011019-025151.

Waskom, M. 2021. "Seaborn: Statistical Data Visualization." *Journal of Open Source Software* 6: 3021. https://doi.org/10.21105/joss.03021.

Wertlen, A. M., C. Niggebrügge, M. Vorobyev, and N. Hempel De Ibarra. 2008. "Detection of Patches of Coloured Discs by Bees." *Journal of Experimental Biology* 211: 2101–2104. https://doi.org/10.1242/jeb.014571.

Westphal, C., R. Bommarco, G. Carré, et al. 2008. "Measuring Bee Diversity in Different European Habitats and Biogeographical Regions." *Ecological Monographs* 78: 653–671. https://doi.org/10.1890/07-1292.1.

Williams, N. M., R. L. Minckley, and F. A. Silveira. 2001. "Variation in Native Bee Faunas and Its Implications for Detecting Community Changes." *Conservation Ecology* 5: art7.

Wilson, J. S., T. Griswold, and O. J. Messinger. 2008. "Sampling Bee Communities (Hymenoptera: Apiformes) in a Desert Landscape: Are Pan Traps Sufficient?" *Journal of the Kansas Entomological Society* 81: 288–300. https://doi.org/10.2317/JKES-802.06.1.

Ye, R., Q. Gao, Y. Qian, J. Sun, and T. Li. 2024. "Improved YOLOv8 and SAHI Model for the Collaborative Detection of Small Targets at the Micro Scale: A Case Study of Pest Detection in Tea." *Agronomy* 14: 1034. https://doi.org/10.3390/agronomy14051034.

Supporting Information

Additional supporting information can be found online in the Supporting Information section. **Data S1:** Bill of Materials (All prices from 2024). **Data S2:** YOLO configuration parameters.